第34卷 第1期 焊 接 学 报 Vol. 34 No. 1
2013年1月 TRANSACTIONS OF THE CHINA WELDING INSTITUTION January 2013

低匹配对接接头形状参数对三点弯曲应力集中系数的影响

王佳杰[1,2]， 董志波[1]， 张敬强[1]， 刘雪松[1]， 方洪渊[1*]
(1. 哈尔滨工业大学 先进焊接与连接国家重点实验室，哈尔滨 150001;
2. 黑龙江工程学院 材料与化学工程学院，哈尔滨 150050)


王佳杰

摘 要: 弹性阶段以提高低匹配接头弯曲承载能力为目标，基于有限单元法针对X形坡口低匹配对接接头三点弯曲形状设计，从材料力学方法角度出发，考察了双侧余高对称时低匹配对接接头的焊缝余高、盖面焊道宽度、焊趾过渡圆弧半径等形状参数对三个危险区弯曲应力集中系数的影响. 结果表明，对母材与焊缝交界处突变区与焊缝底部中心区的影响规律为焊缝余高影响最大，盖面焊道宽度影响次之，焊趾圆弧半径影响最小; 对焊趾部位影响规律为盖面焊道宽度的影响较大，焊趾圆弧半径和焊缝余高影响均较小. 选择合适的形状参数可以提高低匹配接头弯曲承载能力.

关键词: 高强钢; 低匹配对接接头; 接头形状参数; 弯曲应力集中系数
中图分类号: TG404 **文献标识码:** A **文章编号:** 0253-360X(2013)01-0073-04

0 序 言

高强钢焊接时容易出现冷裂纹、焊缝韧性储备不足等问题[1]. 目前主要通过焊前预热、焊后热处理、随焊冲击碾压及采用高强高韧性焊材等措施降低冷裂纹[2-4]. 由于低强匹配焊接能够改善高强钢的可焊性、有效降低拘束应力、降低预热温度或不预热焊接，改善抗裂性能，目前低强匹配设计已得到广泛的重视甚至已纳入相关标准[3,4]，但是低匹配焊接接头因许用应力要相应减少、焊缝发生塑变集中导致接头极限变形能力急剧降低而过早破坏，这无疑降低了低匹配接头承载能力和结构的安全性，难以实用化[5]. 为提高低匹配焊接接头承载能力，相关研究表明[6,7]，通过适当的盖面焊道宽度、余高和焊趾半径等几何形状设计，可提高低匹配焊接接头的承载能力. 王涛等人[8]从断裂力学角度提出使焊缝中心含有裂纹的低匹配对接接头形状参数对承载能力的影响. 国内外对焊接接头弯曲性能的研究多集中于冶金与工艺的角度[9,10]，并未见低匹配接头弯曲承载能力方面的报道. 文中将弯曲应力集中系数作为评定弯曲承载能力的指标，研究X形坡口低匹配对接接头几何形状参数对弯曲应力集中系数的影响，这对于提高低匹配接头弯曲承载能力具有理论和现实的意义.

收稿日期: 2012-04-19
基金项目: 先进焊接与连接国家重点实验室开放课题研究基金资助项目
* 参加此项研究工作的还有刚 铁

1 基本概念及理论

结合材料力学基本知识，在弹性阶段三点弯曲横截面上最大弯曲正应力[11]分别为

$$\sigma_{\mathrm{B}}=\frac{3F_{\mathrm{B}}^{\mathrm{e}}l}{8bt^{2}} \tag{1}$$

$$\sigma_{\mathrm{w}}=\frac{3F_{\mathrm{w}}^{\mathrm{e}}l}{8b(t+h)^{2}} \tag{2}$$

式中: σ_{w}, σ_{B} 分别为焊缝和母材最大弯曲正应力; $F_{\mathrm{B}}^{\mathrm{e}}$, $F_{\mathrm{w}}^{\mathrm{e}}$ 分别为母材和低匹配接头的弯曲载荷; l 为两个辊筒支点之间的距离; b 为板宽; t 为板厚的一半; h 为低匹配接头余高.

低匹配接头的弯曲应力集中系数 K 定义为在相同的弯曲载荷作用下，低匹配接头焊缝弯曲正应力 σ_{w} 与母材弯曲正应力 σ_{B} 的比值，即

$$K=\frac{\sigma_{\mathrm{w}}}{\sigma_{\mathrm{B}}} \tag{3}$$

显然由式(2)与式(3)可知，当 $F_{\mathrm{B}}^{\mathrm{e}}$, $F_{\mathrm{w}}^{\mathrm{e}}$, b, l 不变时，可以通过调整焊缝横截面的 h 来调整 σ_{w}，从而调节弯曲应力集中系数 K.

2 有限元模型的建立

利用大型 MSC. MARC 有限元分析软件，按照国家标准 GB/2653—2008 建立有限元模型，低匹配对接接头形式如图 1 所示，有限元模型如图 2 所示. 试样长度为 170 mm，压头直径为 10 mm，支辊直径为 30 mm，辊筒间距为 40 mm. 接头采用 X 形坡口余高双侧对称，采用四节点平面应变单元. 在应力集中的 3 个危险区(图 1)，即母材与焊缝交界处突变 A 区、焊缝底部中心 B 区、焊趾部位 C 区进行了网格细化处理，最小单元尺寸为 0.01 mm. 母材及焊缝金属建模力学性能参数见表 1.

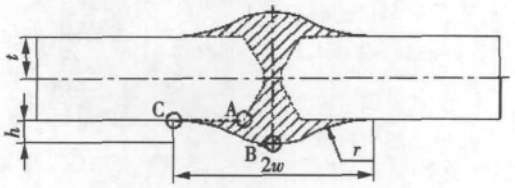

图 1 低匹配对接接头几何参数

Fig. 1 Schematic of geometric parameters for undermatched butt joint

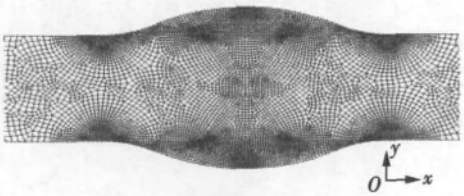

图 2 低匹配对接接头有限元模型

Fig. 2 Finite element model of butt joint

表 1 母材及焊缝金属力学性能

Table 1 Mechanical properties of base metal and weld

	屈服强度 R_{eL}/MPa	断后伸长率 A(%)	弹性模量 E/MPa	泊松比 ν
母材 620-CF	871	19.2	217 800	0.3
焊缝 NJ422	378	35.6	200 000	0.3

3 计算结果及分析

为了分别研究余高高度 h、盖面焊道半宽 w 及焊趾半径 r 三个形状参数中的其中一个参数对弯曲应力集中系数 K 的影响，固定其余两参数. 为简化分析，形状参数 h 及 w 相对板厚做了归一化处理，焊趾半径均选用 $r = 10$ mm.

3.1 焊缝余高对接头应力集中系数的影响

图 3、图 4 及图 5 为盖面焊道相对宽度 w/t 在 1.5 ~ 6.5 范围内变化时，焊缝余高相对厚度 h/t 的变化分别对 K_A，K_B 及 K_C 的影响.

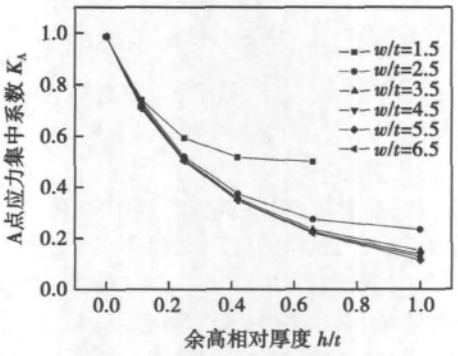

图 3 焊缝余高相对厚度 h/t 对 K_A 的影响

Fig. 3 Influence of relative thickness of reinforcement on K_A

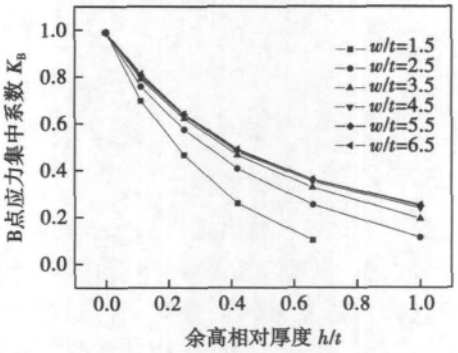

图 4 焊缝余高相对厚度 h/t 对 K_B 的影响

Fig. 4 Influence of relative thickness of reinforcement on K_B

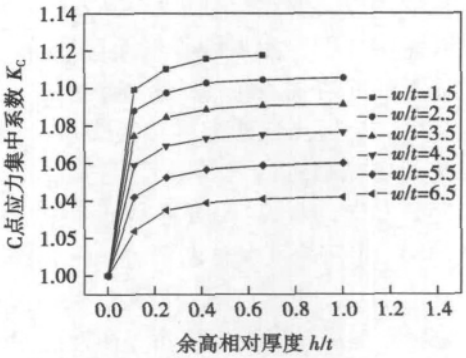

图 5 焊缝余高相对厚度 h/t 对 K_C 的影响

Fig. 5 Influence of relative thickness of reinforcement on K_C

从图 3 可以看出，随 h 的增加，K_A 显著降低. w 越大，随 h 的增加，K_A 降低越显著. 当 h 增大且 w 降低到一定数值时，K_A 将趋于一个稳定值. 从图 4

可以看出，随 h 的增加，K_B 显著降低. w 越小，随 h 的增加，K_B 降低越显著. 从图 5 可以看出，随着 h 的增加，K_C 出现增加的趋势，但是 K_C 变化的范围较小. 在 h 一定的情况下，K_C 随 w 的增加而降低.

3.2　焊缝熔宽对接头应力集中系数的影响

图 6、图 7 及图 8 分别为相对厚度 h/t 在 0 ~ 1.00 范围内时，盖面焊道相对宽度 w/t 的变化分别对 K_A，K_B 及 K_C 的影响.

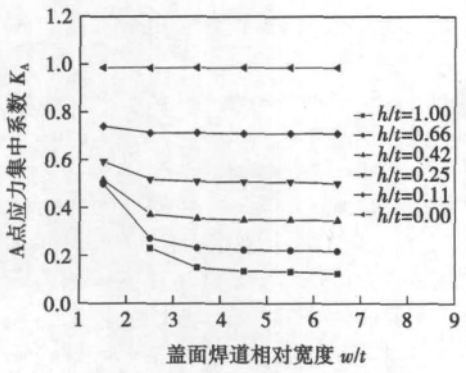

图 6　盖面焊道相对宽度 w/t 对 K_A 的影响

Fig. 6　Influence of relative width of cover pass on K_A

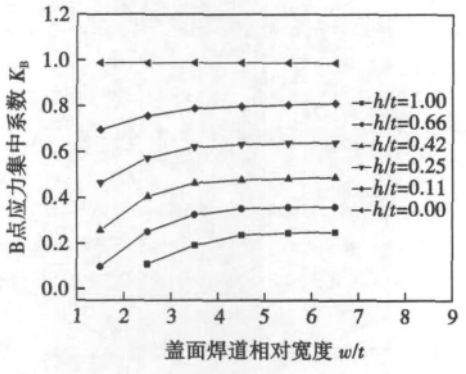

图 7　盖面焊道相对宽度 w/t 对 K_B 的影响

Fig. 7　Influence of relative width of cover pass on K_B

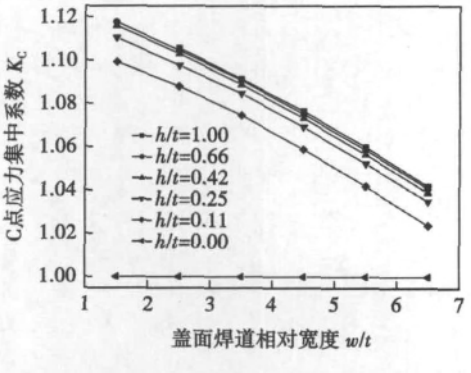

图 8　盖面焊道相对宽度 w/t 对 K_C 的影响

Fig. 8　Influence of relative width of cover pass on K_C

从图 6 中可以看出，当 h 及 r 一定时，K_A 随 w 增加而有所降低，但 K_A 降低的幅度较小. h 越大，K_A 降低越明显. 当 w 足够大时，K_A 将趋于一个稳定值. 从图 7 中可看出，当 h 及 r 一定时，K_B 随着 w 增加逐渐增大，但增大趋势明显减缓. w 一定时，h 越大，K_B 降低越显著. 当 w 足够大时，K_B 将趋于一个稳定值. 从图 8 中可以看出，当 h 及 r 一定时，随着 w 增加，K_C 显著降低.

3.3　焊趾半径对接头应力集中系数的影响

图 9、图 10 及图 11 分别为盖面焊道相对宽度 $w/t=5$，相对厚度 h/t 在 0 ~ 1.00 范围内，焊趾半径 r 的变化对 K_A，K_B 及 K_C 的影响.

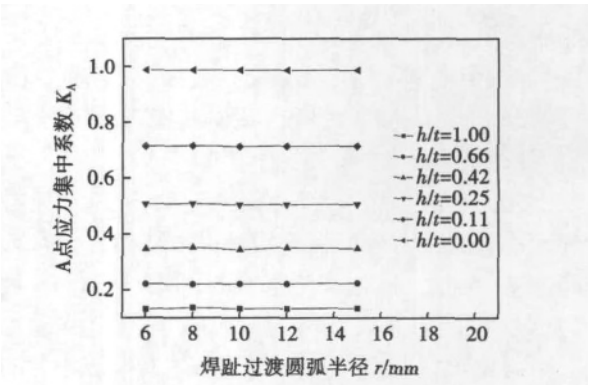

图 9　焊趾半径 r 对 K_A 的影响

Fig. 9　Influence of weld toe radius on K_A

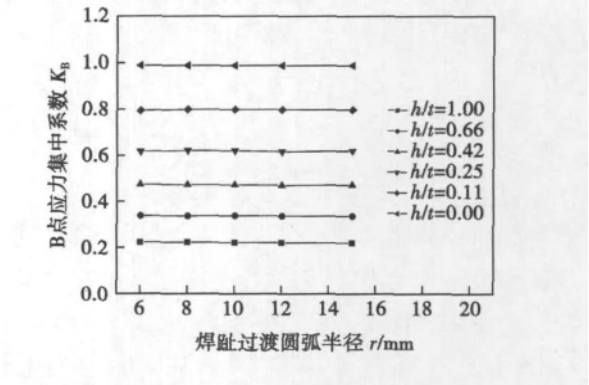

图 10　焊趾半径 r 对 K_B 的影响

Fig. 10　Influence of weld toe radius on K_B

从图 9 及图 10 中可以看出，当 w 和 h 一定时，随着 r 增加，K_A 和 K_B 略有增加，变化范围非常小，所以可以忽略 r 对 K_A 和 K_B 的影响. 从图 11 可以看出，当 h 一定时，随着 r 的增加，K_C 逐渐降低，但降低的幅度较小. 说明在三点弯曲加载中，通过增大焊趾半径实现圆滑过渡，可以使焊趾部位的 K_C 有所降低，但是降低的程度非常有限.

上述分析认为，当 w 一定时，h 对 K_A 与 K_B 的影

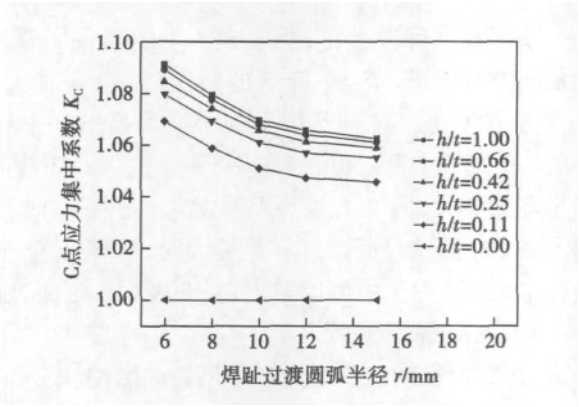

图 11 焊趾半径 r 对 K_C 的影响

Fig. 11 Influence of weld toe radius on K_C

响起着决定性的作用. 由于当 w 一定时,h 越大 A 区与 B 区所在截面的承载面积越大,在弯曲载荷一定情况下,A 区与 B 区所在截面的应力会降低,K_A,K_B 随之降低而 K_C 增大. 但是 w 对 K_A,K_B 及 K_C 出现不同的影响趋势. 当 h 及 r 一定时,w 越大相当于焊缝承载弱化而靠近焊缝的母材承载加强,所以 K_A 降低,K_B 增大. w 越大使得 C 点远离载荷中心而应力迅速降低,从而使 K_C 降低. 由于焊趾部位远离加载中心位置,r 的变化对于 K_A 和 K_B 影响较小,而 K_A 和 K_B 大小主要取决于中心弯曲载荷的大小与所在截面的承载面积. 虽然通过增大 r 可以实现焊趾部位圆滑过渡,使 K_C 有所降低,但是降低幅度非常有限. 因此通过选择合适的焊缝形状参数,可以提高低匹配对接接头弯曲承载能力.

4 结 论

(1) 形状参数对低匹配接头母材与焊缝交界处突变区与焊缝底部中心区弯曲应力集中系数的影响规律为余高影响最大,盖面焊道宽度影响次之,焊趾圆弧半径影响最小.

(2) 形状参数对低匹配接头焊趾部位弯曲应力集中系数的影响规律为盖面焊道宽度影响较大,焊趾半径与焊缝余高高度的影响较小.

(3) 选择合适的焊缝余高、盖面焊道宽度及焊趾半径可以提高低匹配接头的弯曲承载能力.

参考文献:

[1] 刘会杰. 焊接冶金与焊接性 [M]. 北京: 机械工业出版社, 2004.

[2] 黄鲁永. 随焊冲击碾压控制 30CrMnSi 焊接冷裂纹的研究 [D]. 哈尔滨: 哈尔滨工业大学, 2010.

[3] Czyryca E J. Advances in high strength steel technology for naval hull construction [J]. Key Engineering Materials, 1993, 84/85: 491 – 520.

[4] 尹士科, 何长红, 李亚琳. 美国和日本的潜艇用钢及焊接材料 [J]. 材料开发及应用, 2008(2): 58 – 63.
Yin Shike, He Changhong, Li Yalin. Submarine steel and welding consumables used in American and Japan [J]. Development and Application of Materials, 2008(2): 58 – 63.

[5] 张京海, 方大鹏. 高强钢低匹配焊接接头应用性能研究 [J]. 材料开发及应用, 2012(6): 1 – 6.
Zhang Jinghai, Fang Dapeng. Practicability pesearch on low-match weld joint of high-strength steel [J]. Development and Application of Materials, 2012(6): 1 – 6.

[6] 赵智力, 方洪渊, 杨建国, 等. 一种针对低匹配焊接接头的"等承载"设计方法 [J]. 焊接学报, 2011, 32(4): 87 – 90.
Zhao Zhili, Fang Hongyuan, Yang Jianguo, *et al*. A design method of equal load-carrying capacity for under-matching weld joints [J]. Transactions of the China Welding Institution, 2011, 32(4): 87 – 90.

[7] 王佳杰, 董志波, 刘雪松, 等. 弹性阶段低匹配对接接头三点弯曲余高形状设计 [J]. 焊接学报, 2012, 33(8): 37 – 40.
Wang Jiajie, Dong Zhibo, Liu Xuesong, *et al*. Shape design of the reinforcement for under-matched butt joints under the three-point bending load in elastic stage [J]. Transactions of the China Welding Institution, 2012, 33(8): 37 – 40.

[8] 王 涛, 杨建国, 刘雪松, 等. 含中心裂纹低匹配对接接头形状参数对形状因子的影响 [J]. 焊接学报, 2012, 33(1): 101 – 104.
Wang Tao, Yang Jianguo, Liu Xuesong, *et al*. Influence of joint geometric parameters on shape factor of under-matched butt joint with center crack [J]. Transactions of the China Welding Institution, 2012, 33(1): 101 – 104.

[9] 邱葭菲, 曹时增. 20g 埋弧自动焊焊接接头冷弯开裂的研究 [J]. 现代制造工程, 2003(11): 46 – 47.
Qiu Jiafei, Cao Shizeng. Study on cold bend cracking for submerged arc weling joint of 20g [J]. Machinery Manufacturing Engineer, 2003(11): 46 – 47.

[10] Wang Guoqing, Wu Aiping, Zou Guisheng, *et al*. Bending properties and fracture behavior of Ti-23Al-17Nb alloy laser beam welding joints [J]. Tsinghua Science and Technology, 2009, 14(3): 293 – 299.

[11] 刘鸿文. 材料力学(II) [M]. 北京: 高等教育出版社, 2004.

作者简介: 王佳杰,男,1975 年出生,博士研究生,副教授,国际焊接工程师. 主要从事焊接结构可靠性分析和热喷涂教学与科研工作. 发表论文 10 余篇. Email: wangjiajie2006@126.com

Zn)$_6$Sn$_5$, Cu$_6$(Sn, Zn)$_5$ and Cu-Zn solid-solution alloy were formed, among which the Cu-Zn solid-solution alloy layer can greatly affect the diffusion of Cu. Zn served as a diffusing element during the interface reaction, which can improve the unbalanced diffusion of Cu and Sn to a great degree, and suppress the formation of voids effectively.

Key words: Zn; interface; Kirkendall void; intermetallic compound

Stress analysis of plain dent on pipeline based on finite element method WU Ying[1], ZHANG Peng[1], XIE Yanping[2] (1. School of Civil Engineering and Architecture, Southwest Petroleum University, Chengdu 610500, China; 2. Oil and Gas Production Capacity Construction Project, Department of PetroChina Tarim Oilfield, Korla 841000, China). pp 57 – 60

Abstract: For the typical plain dent on pipeline, according to the actual operation situation of the pipeline, the finite element models were established. When other parameters were invariable, a large number of calculations were carried out by changing dent depth, pipe wall thickness, pipe diameter and longitudinal dent length. The calculation results were sorted, inducted, and plotted. On this basis, the results were analyzed by single factor and multiple factors analysis, and then the changing rules between the stress and various parameters were obtained. Non-linear regression analysis was utilized to fit the results. The results show that the relationships between the maximum stress in the dented pipeline, the dent depth, wall thickness, diameter of pipeline, and the longitudinal length of the dent were modeled by sine, index, linear and semi-log liner function, respectively. Some specific expression are obtained in certain range.

Key words: pipeline; plain dent; stress; finite element method; fitting

Study on humping bead formation mechanism in thick-wire high-speed MAG welding YANG Zhanli, ZHANG Shanbao, YANG Yongbo, TANG Qilong* (Harbin Welding Institute, China Academy of Machinery Science & Technology, Harbin 150080, China). pp 61 – 64

Abstract: The humping bead formation mechanism in the thick-wire(ϕ 3.2) high-speed MAG welding process was studied. Using the high-speed camera system, the arc shape and weld pool flow were investigated. By analyzing the captured image, the viewpoint of dynamic equilibrium point was presented. The distance between the dynamic equilibrium point and the arc is the cause of humping bead formation. Any factors to prompt the dynamic equilibrium point to move to the arc, will prevent formation of humping bead. In contrast, any factors to prompt the dynamic equilibrium point away from the arc, will lead to the appearance of humping bead. Furthermore, the uphill and downhill welding experiments were designed to verify the correctness of the above discussion about humping bead formation mechanism.

Key words: humping bead; undercut; molten pool; high speed camera system

Continuous trajectory model of intersecting joint welding robot based on groove feature WANG Tianqi, LI Liangyu, YUE Jianfeng (Tianjin Key Laboratory of Modern Electromechanical Equipment Technology, Tianjin Polytechnic University, Tianjin 300387, China). pp 65 – 68

Abstract: A continuous trajectory mathematical model was established for offshore platform jacket welding robot. The robot with 5 degrees of freedom has enough workspace to finish automatic welding of Y joint and flexibility to meet the requirement for obstacle avoidance in K-joint welding. The kinematics of the robot was built according to the robot structure. Since this robot has a redundant degree of freedom, the joint value was calculated by two steps methods. To ensure the motion stability of the robot, the joint velocity was calculated by derivation operation of joint value through limited method. The simulation result shows that this robot can achieve automatic welding of the K, Y, T joint, and the mathematical model of joint value and velocity can be used to control this robot.

Key words: pipe joint with groove feature; multi-pass welding; offshore platform jacket

Design of human-machine interactive robotic arc welding remanufacturing system YIN Ziqiang[1,2], ZHANG Guangjun[2], ZHAO Huihui[2], YUAN Xin[1], WU Lin[2] (1. Institute of Oceanographic Instrumentation, Shandong Academy of Sciences, Qingdao 266001, China; 2. State Key Laboratory of Advanced Welding and Joining, Harbin Institute of Technology, Harbin 150001, China). pp 69 – 72

Abstract: On the basis of analyzing the characters of the worn parts, a novel remanufacturing solution was proposed. The remanufacturing of the worn parts was realized by a human-machine interactive remanufacturing system based on robotic GMAW. The system takes operators as the intelligent factor to solve the complicated problems of the system, which are nonlinear and hard to model. The computer and machine were employed to solve the high speed and high accuracy problem, for instance the numerical computation and motion control etc. After the experiment system platform being established, the structure of the system software and the human-machine interactive scheme were studied, and the visual human-machine interface was designed by modularized program.

Key words: human-machine interactive; robotic arc welding; remanufacturing; off-line programming

Influence of joint geometric parameters on stress concentration factor for under-matched butt joint under three-point bending load WANG Jiajie[1,2], DONG Zhibo[1], ZHANG Jingqiang[1], LIU Xuesong[1], FANG Hong yuan[1*] (1. State Key Laboratory of Advanced Welding and Joining, Harbin Institute of Technology, Harbin 150001, China 2. School of Materials and Chemical Engineering, Heilongjiang Institute of Technology, Harbin 150050, China). pp 73 – 76

Abstract: In order to improve the bending load-carrying capacity (BLCC) for under-matched butt joints in the elastic stage, the influence of joint geometric parameters on bending stress concentration factor (BSCF) for under-matched butt joint with X-type groove and double side symmetrical type reinforcement was studied based on the finite element method from the viewpoint of materials mechanics. The influence rules of joint geometric parameters on BSCF at the geometric mutations area near fusion line and in the weld bottom center show that the reinforcement plays the most important role in BSCF, the cover pass width has relatively great effect on BSCF and the weld toe radius has

minimal effect on BSCF. The influence rules of joint geometric parameters on BSCF at the weld toe show that the cover pass width has some influence on BSCF, the reinforcement and the weld toe radius both have little influence on BSCF. BLCC of under-matched butt joint can be improved by choosing appropriate joint geometric parameters.

Key words: high strength steel; under-matched butt joint; joint geometric parameters; bending stress concentration factor

Effect of sulphur on silver filler metal and brazing properties ZHANG Guanxing[1], LONG Weimin[1], BAO Li[1], SUI Fangfei[2] (1. State Key Laboratory of Advanced Brazing Filler Metals, Zhengzhou Research Institute of Mechanical Engineering, Zhengzhou 450001, China; 2. School of Materials Science & Engineering, Zhengzhou University, Zhengzhou 450001, China). pp 77 - 80

Abstract: The properties of sulphurized silver based solder were studied by optical microscope, scanning electron microscopy and other analytical tools. The experimental results indicate that the tensile strength of sulphurized filler metal decreased significantly, and then to a certain extent until not varied. The difference of wettability was obvious at different sulphurizing time. The wetting area was reduced by nearly half at the sulphurizing time of 30 min, but the wetting area of brazing filler metal would change little if the sulphurizing time further lasted. Relative dense sulphurized layer was formed on the surface of brazing filler metal and its thickness was about 10 μm. The distribution of Zn and Cu in the sulphurizing layer and the internal brazing filler metal is relatively uniform, while the Ag element is distributed periodically. Sulfur existed in the form of Ag_2S, Cu_2S, CuS and ZnS in the brazing filler metal. The melting points of Ag_2S, Cu_2S, CuS and ZnS were relatively high, and their existence would affect the welding properties severely.

Key words: sulfurizing; wettability; tensile strength; sulfide

Effects of laser micro-joining on microstructure and corrosion resistance of glass-ceramic coatings CHEN Pinghu[1], QIU Changjun[1], CHEN Yong[2], LONG Chongsheng[3] (1. School of Mechanical Engineering, Nanhua University, Hengyang 421001, China; 2. College of Materials Science and Engineering, Chongqing University, Chongqing 400030, China; 3. Nuclear Power Institute of China, Chengdu 610041, China). pp 81 - 84

Abstract: The high-temperature sintering and ball milling were adopted to prepare SiO_2 glass and Cr_2O_3 ceramic composite powder. The glass-ceramic coating was prepared by using the high-velocity flame spraying on the surface of 45 steel. And laser micro-joining techniques were used as secondary treatment in order to improve its properties. Effect of laser micro-joining on microstructure and properties of glass-ceramic coatings were investigated. The results showed that the laser micro-joining method being taken as the secondary treatment, the compactness of the coating is improved and the coatings becomes more uniform, and the micropores and crack in the glass-ceramic coating are reduced; the bonding strength of the interface, hydrophobic properties and corrosion resistance of the coatings are enhanced obviously. Consequently, the comprehensive performance of the glass-ceramic coatings is dramatically enhanced when laser micro-joining is adopted as the secondary treatment.

Key words: glass-ceramic coatings; laser micro-joining; hydrophobic properties; corrosion resistance; bonding strength

Effect of alloy elements on microstructure and phase structure of laser cladding Fe-based coatings NIE Binying[1], YAO Chengwu[2] (1. Chemical and Biological Engineering College, Yichun University, Yichun 336000, China; 2. Shanghai Key Laboratory of Materials Laser Processing and Modification, Shanghai Jiaotong University, Shanghai 200240, China). pp 85 - 88

Abstract: Four types of Fe-based alloys were fabricated on 45 carbon steel substrate by CO_2 laser surface cladding, and the effect of alloy elements on the microstructure and carbides of the coatings was investigated. With the increasing of the elements V, Nb, Ti, CeO in turn, the structure of the coating was transformed from the columnar crystal to columnar dendrites, and finally to the dendrite. With the simultaneous addition of the two elements V, Nb in the coating, the long strip carbides in the interdendritic region split into blocky carbides. At last, the carbides in the interdendritic region of the coating can be refined and spheroidized by adding elements V, Nb, Ti, CeO. The tensile test results showed that the tensile strength and elongation rate of the coating with dendritic structure and spheroidized carbides in the interdendritic region increased greatly, and the coating had high strength-toughness properties.

Key words: laser cladding; Fe-based alloy; alloy elements; microstructure morphology; carbides

Fracture characteristic of fiber laser-arc hybrid welded joints of 400 MPa grade ductile cast iron ZHENG Shiqing[1], LIU Zhu[1], SHAN Jiguo[1,2], WEN Peng[1,2] (1. Department of Mechanical Engineering, Tsinghua University, Beijing 100084, China; 2. Key Laboratory for Advanced Materials Processing Technology, Ministry of Education, Tsinghua University, Beijing 100084, China). pp 89 - 92

Abstract: Laser-MIG arc hybrid welding was used to weld 400 MPa grade ductile cast iron, which is used on key parts of wind power. The thickness of base metal is 5 mm, and 308L stainless steel wire was used as filler wire. The welds with good appearance and full penetration were obtained, and then the influence of welding conditions on tensile properties and fracture characteristic of joints was studied. The results show that the joint at low arc heat input has low tensile properties, fracture expands along the fusion line and it is brittle; the joint at high arc heat input has high tensile properties, fracture expands along base metal, which is brittle on the top of the joint and flexible at the bottom of the joint. The difference of joints fracture characteristic is caused by different quantities of ledebutire at the bottom of fusion zone and partial melting zone (PMZ) of the joints. Based on previous research results, a joint with the tensile strength of 346.4 MPa, the elongation of 5.4% was obtained and its fracture expands along base metal.

Key words: fiber laser-MIG arc hybrid welding; ductile cast iron; fracture characteristic; arc heat input

Corrosion resistance of different particle-density WC-10Co-4Cr coatings DING Kunying, CHENG Taotao, WANG